



6-4-23

## EXPERIMENTAL STUDY ON DEGREE OF FIXATION AT PILE HEAD JOINT AND FAILURE STRENGTH OF PRESTRESSED HIGH STRENGTH CONCRETE PILES

Yoshihiro SUGIMURA<sup>1</sup> and Tsutomu HIRADE<sup>2</sup>

<sup>1</sup>Professor, Department of Architecture, Tohoku University,  
Sendai, Japan

<sup>2</sup>Research Engineer, Geotechnical Engineering Division, Building  
Research Institute, Ministry of Construction, Tsukuba, Japan

### SUMMARY

Experimental result of full-scale bending-shear tests on joints between prestressed high strength concrete (PHC) pile and footing under various axial load conditions are discussed to investigate degree of fixation at pile head and the ultimate strength. Conclusions are classified into the followings: 1) Degree of fixation at pile head is affected significantly by embedding length of pile into footing and axial load. 2) Final state of PHC pile results in shear failure type, especially in axial load condition, so that it is important to make an effort to keep its ductility in the ultimate capacity design.

### INTRODUCTION

In the earthquake resistant design of pile foundation, it is important to accumulate information about degree of fixation, i.e., degree of restraint for rotation at pile head and the ultimate strength of pile. Theoretical solutions of horizontal resistance of pile are discussed by introducing the concept of degree of fixation at pile head and effect of pile length in the previous paper (Ref. 1). In succession, this paper discusses experimental results of full-scale bending-shear tests for joint between prestressed high strength concrete pile and footing under various axial load conditions, in order to investigate degree of fixation at pile head joint and the ultimate strength of piles.

### OUTLINE OF EXPERIMENTS

Test Program Statically indeterminate loading system is used as shown in Fig.1, which is capable of keeping the similarity of bending moment distribution of pile in the ground due to horizontal force. The loading points B, C, and the supporting point A are treated as free for rotation by using teflon lubricant device support. Footing is fixed to the floor of test room by using the two PC bars. Each value of loading step  $P_a$ ,  $P_{cr}$  and  $P_u$  corresponding to the allowable, the design crack and the design failure bending moment of pile, is calculated for the case that pile head joint is assumed to be completely fixed. And, in principle, after repeating 3 cycles, 5 cycles, and 1 cycle at these loading steps, load is increased to the final failure state. Experiments are performed in the two phase test series as shown in the following sections.

Test Specimens An example of test specimen is shown in Fig. 2, for the case of 20Z'. Pile sections and details of pile head joint in phase 1 test series are

shown in Fig. 3 and Fig. 4, respectively. And concrete strength of each specimen is shown in Table 1. Twenty four test specimens, in total, are selected by combining pile diameters of 35 cm and 50 cm, pile grades of A (effective prestress:  $\sigma_e=40 \text{ kg/cm}^2$ ) and C ( $\sigma_e=100 \text{ kg/cm}^2$ ), and axial loads of 0, 30 and 60 t. The detail of joint method in phase 1 test series are as follows. Type X is the most common method that pile cut together with PC bars is buried simply in footing with 10 cm depth, and plain concrete is filled inside of pile up to length corresponding to pile diameter. Type Y is the same method as type X except that reinforced concrete is filled inside of pile with a little longer length. Type Z is the method that pile cut leaving PC bars 50 times as long as those diameter is buried in footing with 10 cm depth, and covered by steel pipe with concrete outside and filled with plain concrete inside of pile to 40 cm long from pile top.

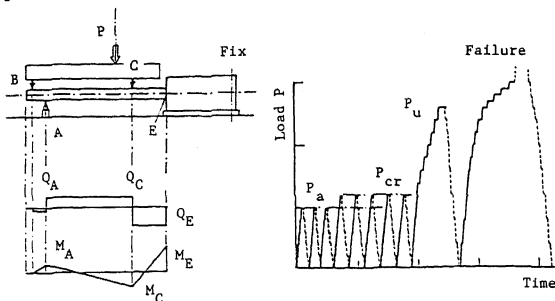


Fig. 1 Outline of loading system

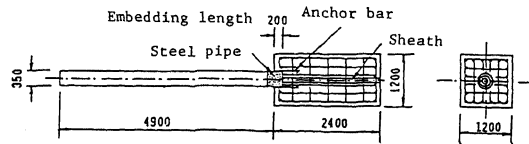


Fig. 2 Test specimen (case 20Z')

The types of test specimen and strength of materials in phase 2 test series are shown in Table 2 and Table 3, and section of pile and detail of pile head joint are shown in Fig. 5 and Fig. 6. In this case, piles in 35 cm diameter of grade B ( $\sigma_e=80 \text{ kg/cm}^2$ ) are used for supplement of phase 1 test series. The piles were manufactured with separator at the pile end and cut the outer part of PC bars after curing, in order to estimate relaxation of prestress due to cut off of pile head at sites. Change of prestress during this process was measured by strain gages set up on PC bars and these measured values are listed in Table 2 as the measured effective prestress. Axial load during tests is 30 t in all the cases.

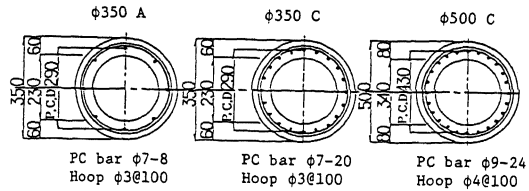


Fig. 3 Pile section (phase 1 series)

Similar three types of joint method, i.e., X', Y' and Z' are selected in phase 2 test series, but by using three different embedding lengths in order to investigate effects of embedding. The type X' is the same method as type X in phase 1 test series, but two kinds of embedding length are selected, i.e., 10 cm and 35 cm, which are called as test specimens 10X' and 35X', respec-

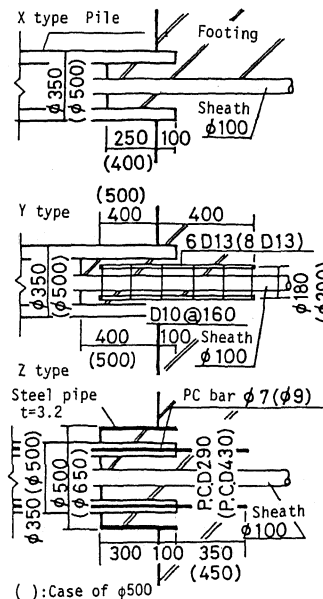


Fig. 4 Detail of pile head joint (Phase 1 series)

Table 1 Properties of test specimen (phase 1 series)

Test No.	Pile		Footing	
	$F_c$	$t$	$F_c$	$E_c$
35AX00	884	64	244	2.45
35AY00	884	64	207	2.52
35AZ00	903	65	178	2.34
35AX30	884	63	247	2.61
35AY30	884	63	233	2.55
35AZ30	903	67	224	2.45
35AX60	884	60	226	2.71
35AY60	884	60	199	2.63
35AZ60	860	65	184	2.68
35CX00	902	65	268	2.44
35CY00	902	65	233	1.86
35CZ00	888	66	194	1.97
35CX30	887	62	204	1.64
35CY30	887	65	212	1.86
35CZ30	888	69	170	1.68
35CX60	886	69	261	2.55
35CY60	886	65	234	2.30
35CZ60	888	65	226	2.12
50CX00	954	83	198	2.82
50CY00	954	84	187	2.41
50CZ00	901	88	175	2.71
50CX60	954	84	177	2.50
50CY60	954	83	223	2.44
50CZ60	901	84	171	2.33

$F_c$ :  $\text{kg/cm}^2$   $t$ :  $\text{mm}$   $E_c$ :  $\times 10^5 \text{ kg/cm}^2$

Table 2 Properties of test specimen (phase 2 series)

Test No.	Thick-ness t (cm)	Equivalent moment iner. $I_e$ (cm <sup>4</sup> )	Effective prestress $\sigma_e$ (kg/cm <sup>2</sup> )	Design bending moment	
				$M_a$ (tm)	$M_{cr}$ (tm)
10X'	6.77	65940	87.09	6.67	7.99
10Z'	6.94	66590	86.17	6.67	8.00
20Z'	6.42	64520	95.33	6.91	8.20
20Y'	6.15	63320	94.91	6.83	8.10
35X'	7.75	69260	80.50	6.56	7.94
Standard	6.00	62620	80.00	6.17	7.42

Table 3 Properties of materials (phase 2 series)

Steel (kg/cm <sup>2</sup> )				Concrete (kg/cm <sup>2</sup> )			
Diameter (mm)	$\sigma_t$	$\sigma_y$	$E_s \times 10^5$	No. (day)	$F_c$	$E_c \times 10^5$	
PC bar	9.2	15255	13400	2.11			
Footing	D13	6350	4455	2.00	File	49	895
Anchor	D10	5762	3814	2.01	10X'	35	228
					10Z'	35	226
					20Z'	34	231
					20Y'	34	235
					35X'	33	237

$\sigma_t$ : Tension     $\sigma_y$ : Yield  
 $F_c$ : Comp.     $E_s, E_c$ : Young's modu.

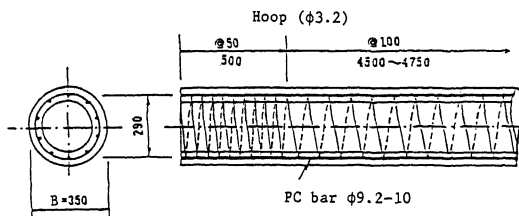


Fig. 5 Pile section (phase 2 series)

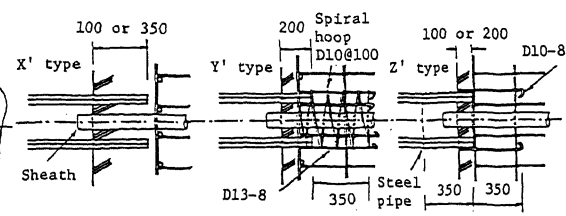


Fig. 6 Detail of pile head joint (phase 2 series)

tively. Type Y' is the method pile head in footing is reinforced by rising steel bars and spiral hoops with embedding length of 20 cm which is called as test specimen 20Y'. In this case, reinforcing cage is not unified with pile. Type Z' is the similar method as type Z, but steel pipe (inner diameter: 35.4 cm, length: 35 cm, thickness: 0.6 cm) is glued to pile with epoxy resin, and 8 anchor steel bars of 35 cm bond length (D10-8) are welded to steel pipe. Embedding length are selected as 10 cm and 20 cm which are called as test specimens 10Z' and 20Z', respectively. In all the specimens in phase 2 test series, plain concrete is not filled inside of pile below the footing.

The size of footing and ratio of reinforcement is basically common in both test series, except that the eight steel bars are bended downward and binded to steel pipe pile for the case of Z' type, and are bended upward around pile surface for the case of Y' type. The shortest distance from the center of pile section to the side of footing is about 1.7 times as long as pile diameter in the case of 35 cm pile diameter, and 1.2 times in the case of 50 cm pile diameter.

**Measurement Program** The followings are measured in both test series: 1) loads at points B and C, and reaction force at point A for determination of bending moment distribution of pile, 2) displacements at points B, C, A and at pile head joint E for getting of deflection of pile, 3) angle of rotation at pile head, 4) angle of rotation of footing, 5) strains at pile surface for checking of bending moment distribution of pile.

## TEST RESULTS

**Load-Deflection Curve** Figure 7 shows envelope curves of the maximum displacement of pile at the virgin loads in phase 2 test series. It is noticed that the maximum displacement occurs at some distance from the point C and the slight displacement is also observed both at the point A and the pile head joint E. The maximum load is the largest for the case of 35X', and becomes smaller in the order of 10Z' > 10X' > 20Z' > 20Y' within the range from 27.3 t to 34.9 t. And the corresponding displacement of pile is scattering in the range from 2 to 4 cm,

changing smaller in the order of 35X' > 10X' > 10Z' > 20Y' > 20Z'.

Degree of Fixation at Pile Head at the Allowable Bending Moment of Pile Figure 8 shows comparison of the degree of fixation at pile head  $\alpha_r$  in each test when the bending moment of pile reaches its allowable value. The abscissa is the ratio between embedding length of pile into footing and pile diameter  $\alpha_d$ , and the part of outer steel pipe pile is included in the embedding length for the case of joint type Z. The ordinate is the degree of fixation at pile head, which is corrected to avoid the effect of rotation of footing  $\theta_F$  and displacement at the point E and A by the following equations (see Fig. 9).

$$\alpha_r = M_E' / M_{E_f} \quad (1)$$

$$M_E' = M_E - \Delta M_E \quad (2)$$

$$= M_E - 3EI (\ell \theta_F + y_E - y_A) / \ell^2$$

$$M_{E_f} = [cP_1 - ab(\ell+a)P_2 / \ell^2] / 2 \quad (3)$$

in which,  $M_E$  is the bending moment at the point E determined by the loads  $P_1$ ,  $P_2$  and the reaction force  $R_A$ ,  $\Delta M_E$  is the influence component to  $M_E$  determined by the angle of rotation of the footing  $\theta_F$ , and the displacements  $y_E$  and  $y_A$ .  $M_{E_f}$  is the theoretical bending moment at the point E corresponding to the conditions of pin support at the point A and fixed joint at the point E, and  $EI$  is the bending rigidity of pile. The following characteristics are derived from Fig. 8. 1) Embedding length of pile into footing is one of the most important influence factor on degree of fixation at pile head  $\alpha_r$ , and  $\alpha_r$  becomes larger as embedding length is longer. When the ratio of embedding length to pile diameter  $\alpha_d$  changes from 0.2 to 1.0,  $\alpha_r$  increases from 0.7 to 0.9, and from 0.4 to 0.75 in average, under the conditions with and without axial load, respectively. If  $\alpha_d$  is nearly equal to 1, condition of pile head becomes similar to rigid joint. 2) The range of  $\alpha_r$  due to the condition with or without axial load has width of about 0.2, respectively, but can be divided clearly into the two groups, i.e., the lower region without axial load and the higher region with the influence of axial load.

Failure Type and the Ultimate Strength of Pile Test results at the maximum load and failure type of each test are summarized in Table 4, and some example of the final states are shown in Fig. 10. In almost all the cases, final state results in shear failure of pile except the cases of pile of

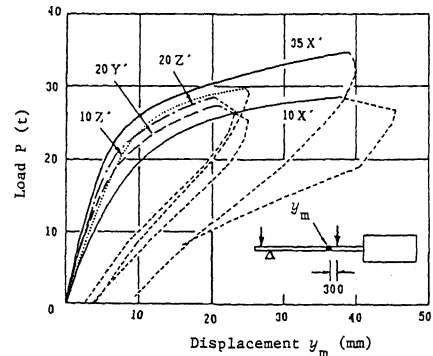


Fig. 7 Relation between load and displacement of pile (phase 2 series)

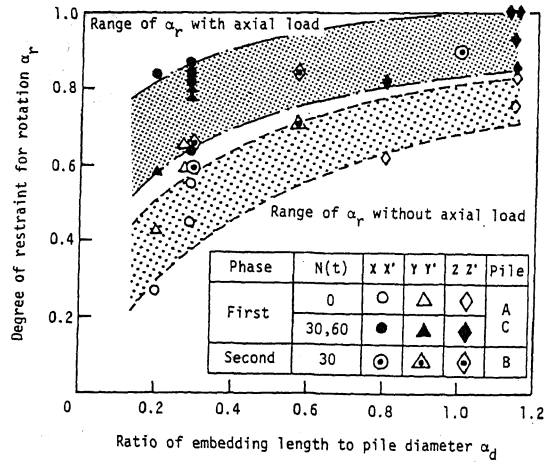


Fig. 8 Degree of restraint for rotation at pile head

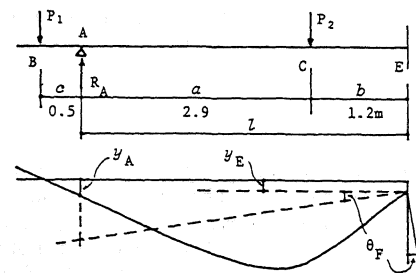


Fig. 9 Correction of bending moment at pile head

grade A without axial load which are determined by bending failure (break of PC bars). As for footing, comparatively large cracks develop in the case of short embedding length but small or no cracks in the case of long embedding length. And, if embedding part is reinforced by spiral hoops, effect of preventing cracks of footing is exhibited.

Figure 11 shows the comparison between experimental and analytical values of shear strength of pile. Analytical values are calculated by the following equations, based on the measured values of pile section and strength of materials.

$$\text{cal } Q_{cr} = (tI/S_0) \sqrt{(\sigma_g + 2\phi\sigma_t)^2 - \sigma_g^2} \quad (4)$$

$$\sigma_g = N/A_e + \sigma_e \quad (5)$$

in which,  $t$  is the thickness of pile,  $S_0$  and  $I$  are the geometrical moment of area and moment of inertia of pile.  $N$  and  $A_e$  are the axial load and equivalent area of pile

Table 4 Values and failure type at the maximum load

No.	P(t)	Q <sub>E</sub> (t)	M <sub>C</sub> (cm)	M <sub>U</sub> (cm)	RBM*	SSR**	Type
35AX00	17.12	-10.28	10.82	-1.42	1.72	3.01	B
35AY00	21.14	-11.97	14.52	0.25	2.30	3.47	B
35AZ00	24.02	-16.65	8.51	-11.37	1.80	1.95	S
35AX30	28.38	-18.57	11.83	-10.36	1.19	1.82	SB
35AY30	25.86	-16.95	12.00	-8.24	1.20	2.02	S
35AZ30	30.38	-20.70	10.39	-14.35	1.44	1.98	S
35AX60	31.40	-20.63	14.11	-10.55	1.06	1.95	S
35AY60	30.74	-20.61	12.69	-11.95	0.96	1.76	S
35AZ60	34.16	-23.38	11.49	-16.47	1.24	2.01	S
35CX00	31.20	-17.82	19.96	-1.32	1.47	3.20	S
35CY00	28.60	-18.16	13.52	-8.18	0.99	2.13	S
35CZ00	33.00	-21.43	14.95	-10.67	1.10	1.99	S
35CX30	32.58	-20.71	16.10	-8.65	0.98	2.22	S
35CY30	29.62	-19.16	13.08	-9.81	0.80	1.95	S
35CZ30	34.14	-22.60	14.93	-12.09	0.91	1.89	S
35CX60	35.28	-22.90	16.04	-11.34	0.85	2.00	SP
35CY60	32.26	-20.80	15.16	-9.79	0.82	2.07	SP
35CZ60	38.48	-25.67	15.69	-15.01	0.84	1.75	SP
50CX00	65.56	-39.06	40.42	-6.26	1.10	2.07	S
50CY00	61.36	-37.81	34.90	-10.28	0.95	1.85	SP
50CZ00	72.16	-45.64	36.89	-17.69	1.00	1.62	SP
50CX60	74.16	-45.96	39.69	-15.26	0.88	1.73	SP
50CY60	70.20	-44.05	36.29	-16.38	0.80	1.65	SP
50CZ60	83.64	-54.09	38.64	-26.07	0.86	1.43	SP
10X'	28.65	-18.46	14.76	-6.17	0.94	2.42	S
10Z'	29.76	-18.85	14.83	-6.86	0.98	2.34	S
20Z'	27.51	-19.45	10.75	-10.12	0.71	1.77	S
20Y'	27.38	-17.36	12.55	-7.06	0.82	2.20	S
35X'	34.88	-22.95	16.68	-8.58	1.07	2.26	S

\*RBM=|Max(M<sub>C</sub>,M<sub>U</sub>)/M<sub>UC</sub>| M<sub>UC</sub>: Analyzed ultimate bending capacity  
 \*\*SSR=|Max(N<sub>C</sub>,N<sub>E</sub>)/(Q<sub>E</sub>\*B)| : Shear span ratio S:Shear  
 B:Bending SB:Shear-bending SP:Shear and pipe bending

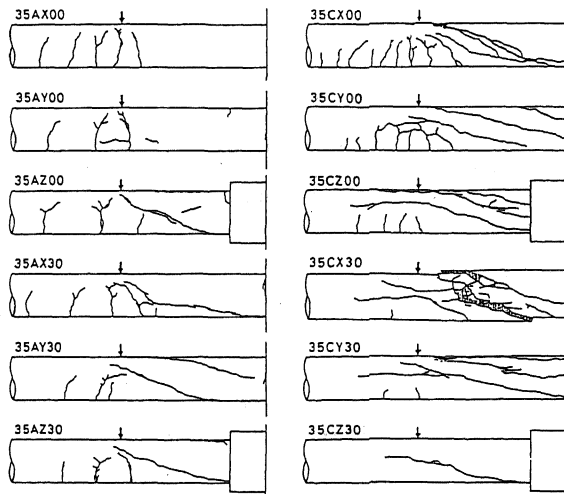


Fig. 10 Examples of the final state of pile (phase 1 series)

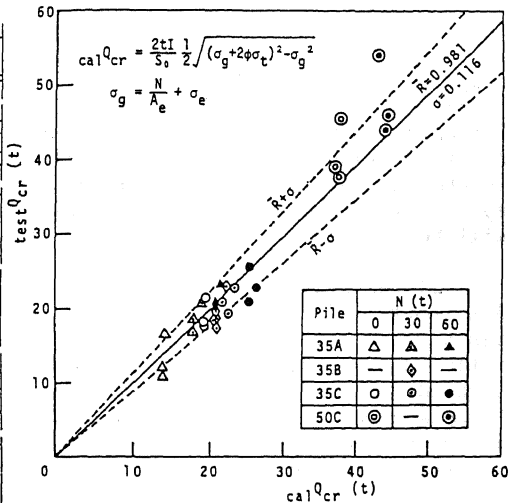


Fig. 11 Comparison between experimental and analytical results of shear strength of pile

section.  $\sigma_e$  is the effective prestress and  $\sigma_t$  is the tensile strength of concrete assumed as 7% of compressive strength.  $\phi$  is the correction factor of shear force assumed to be equal to 0.5. The mean value  $\bar{R}$  and standard deviation  $\sigma$  are 0.981 and 0.116, respectively, as shown in Fig. 11. It should be noticed that eq. (4) overestimates shear strength of pile in some cases. Y. Gotoh and T. Shibata pointed out the accuracy of eq. (4) is slightly inferior to the experimental equation developed by them for estimation of shear strength of reinforced concrete column (Ref. 2).

Table 4 shows also the ratios RBM between experimental and analytical results on the ultimate bending moment of pile. As for  $M_{UC}$  in phase 2 test

series, all the parameters are the measured values except that  $\sigma_t$  is assumed. It should be noted, therefore, that the accuracy is different in each test series and fairly high values of RBM are observed especially in the case of pile grade A without axial load condition. But, on the whole, the values of RBM less than 1 are recognized in many cases, i.e., shear failure of pile precedes the occurrence of bending failure. This tendency is more remarkable for the case with axial load than without axial load. And the test result also explains well the cause of the typical shear-failure-type damage of piles which supported a 11 storied building due to the Miyagiken-oki earthquake in 1978 (Ref. 3). That is to say, the difference of fixation degree of pile head was produced and caused the concentration of horizontal shear force to the piles in compression side because of rocking vibration of the building. And then the piles resulted in shear failure, while the piles in pullout side remained in the state of no damage or slight bending cracks. The importance of design philosophy to avoid the preceding of shear failure of pile will be increasing more and more in earthquake resistant design of pile foundation. Therefore, it is advisable to design leaving sufficient surplus of shear strength of pile, if the eq. (4) is adopted in design process.

### CONCLUSIONS

The conclusions applicable to practical design of pile foundation derived from the foregoing tests are as follows.

1) The important influence factors on degree of fixation at pile head  $\alpha_r$  in the allowable capacity design, are the embedding length of pile into footing and the condition with or without axial load. If pile is embedded to the length corresponding to pile diameter, behavior of pile head becomes similar to rigid joint. And if axial load acts, degree of fixation becomes large entirely. During an earthquake, piles have experience of additional alternating axial load due to rocking motion of superstructure. Therefore, degree of fixation of piles located at compression side becomes larger than pullout side, and shear force is apt to be concentrated to piles in compression side. This effect of axial load will become very important factor for design method of pile foundation.

2) The final state of each test specimen, except some of the piles in grade A without axial load results in shear failure type. Shear span ratios in these tests are scattering in the range from 1.43 to 3.20. Although real shear span ratio of pile in the ground under horizontal force is necessary to be investigated separately, this result explains well the damage type of piles due to the Miyagiken-oki earthquake in 1978 and also proves that the shear strength of pile is indispensable factor in earthquake resistant design. And it is advisable to keep sufficient ductility for the case of PHC pile.

### REFERENCES

1. Sugimura, Y., Theoretical Solutions on Horizontal Resistance of Pile by Considering Degree of Restraint for Rotation at Pile Head and Pile Tip (in Japanese), Jour. of Struct. and Construc. Eng., Trans. of AIJ, No.365, 132-143, (1986)
2. Gotoh, Y. and Shibata, T., Shear Strength Estimation for Pretensioned Spun High Strength Concrete Piles (in Japanese), Annual Meeting of AIJ, 983-984, (1985)
3. Sugimura, Y., Earthquake Damage of Pile Foundation in Japan, Discussion on Soil Dynamics and Geotechnical Aspects of Earthquake Engineering, Proc. of the 8th ARCSMFE, 2, 245-246, (1987)